ENTROPY PRODUCTION IN PERISTALTIC FLOW OF A SPACE DEPENDENT VISCOSITY FLUID IN ASYMMETRIC CHANNEL

Najma SALEEM

Department of Mathematics and Natural Sciences, Prince Mohammad Bin Fahd University, Khobar, 31952 Saudi Arabia
Email: nsaleem@pmu.edu.sa

Abstract: *In this article, second-law analysis has been made for the peristaltic flow of a viscous variable viscosity fluid in an asymmetric channel. The entire study is carried out in a moving frame of reference. The exact solutions of the problem have been obtained by normalizing the governing equations. The main sources of entropy generation in the peristaltic flow have been investigated. Graphical illustrations of the total entropy generation number and the Bejan number have been provided and effects of pertinent parameters of interest are discussed. It is established that the entropy generation is minimum in the expanding region of the channel. Moreover, the entropy generation rises in the cooled region of the channel by increasing the variable viscosity parameter.*
Keywords: *Entropy generation; Peristaltic flow; asymmetric channel; Variable viscosity fluid*

1. Introduction

Peristaltic process is an automatic series of muscle waves of contraction and expansion that occurs in digestive system to move the food stuff through digestive tract. It also plays a key role in moving urine from kidneys to the bladder, movement of eggs and sperms in male and female reproductive systems and bile from gallbladder into the duodenum and so on. Peristaltic motion is considered to be the normal function of body and it can be seen in abdomen when gas moves along. Peristaltic pumps are designed by following the peristaltic motion principal. These are used to pump a variety of clean and aggressive fluids in order to avoid their contamination with exposed pump components. Similarly this mechanism is also very common in other biological and biomedical systems, chemical industries and laboratories. Due to its physical importance in human life applications, it has become a charming field of research since last few decades. It was Latham [1] who presented his first experimental and theoretical effort towards peristalsis. After then Shapiro *et al.* [2] introduced the conditions of large wavelength and small Reynolds number for inertial effects to be negligible and for the pressure to be considered uniform over the whole cross-section. A frequently occurring geometrical situation is asymmetrically moving waves of channel walls. In this regards, Eytan and Elad [3] examined the peristaltic transport resulting from symmetric and asymmetric contractions for various displacement waves on the channel walls. They concluded that transport phenomenon is strongly controlled by amplitude and phase shift of wall displacement from both channel walls. A similar sort of study was conducted by Srinivas and Pushparaj [4] who examined

peristaltic transport of an MHD viscous fluid in an inclined planar asymmetric channel. A peristaltic flow of non-Newtonian Casson fluid flowing in asymmetric channel was investigated by Naga Rani and Sarojamma [5]. Mishra and Rao [6] have observed the peristaltic transport of incompressible viscous fluid in a channel conserving the peristaltic waves with different amplitude and phase and noticed that reflux and trapping increases from asymmetric to symmetric situation. Later on, Hayat *et al.* [7] scrutinized the peristaltic motion in asymmetric channel by considering Carreau fluid. They commented that axial velocity of Carreau fluid increases with a decrease in phase difference and increase in mean flow rate. Heat transfer analysis is also a vital part in investigating the peristaltic flows for biological systems and biochemical processes as well. In the process of digestion a most important phenomenon is the metabolism. One type of metabolism is called catabolism which is the breakdown of the complex molecules into small units to produce energy. The first-law of thermodynamics defines the starting and ending point of this process. The second law of thermodynamics accompanied by the phenomenon of entropy also has high significance in this process. This procedure increases the order in the body and thus reduces entropy. Though, human body transfers heat to the entities with which it contacts in form of conduction. Additionally, it generates convection due to the change in the temperature of body and the environment and radiates heat into space, exhausts energy-comprising substances in the form of food, and excretes waste in the form of carbon dioxide, water, breath, urine and feces. Consequently, the overall entropy of the human body system rises. The growth of entropy in human body affects biological fluids inside body, such as, blood flow, urine passage from kidney to bladder through ureter, lymph movement in lymphatic vessels, sperm transportation, swallowing food through esophagus, etc. Some interesting heat transfer studies in peristalsis flows can be found in Sarkar *et al.* [8], Akbar *et al.* [9] and Sher Akbar *et al.* [10])

The phenomenon of entropy was initially studied by Bejan [11] in four different convective heat transfer configurations. An attempt was made by Bejan [12] to minimize the entropy generation of an engineering system by an efficient thermal design. Bejan [13] introduced the phenomenon of entropy generation minimization EGM to optimize the thermal design and efficiency of thermodynamical systems. In which he disclosed the two major sources of entropy production in a system; the heat transfer rate and the viscous effects in fluid. After this groundbreaking work of Bejan numerous researchers (Arikoglu *et al.* [14], Tamayol *et al.* [15], Butt *et al.* [16], Erbay *et al.* [17], Abu-Hijleh and Heilen [18], Tasnim *et al.* [19], Eegunjobi *et al.* [20], Adesanya and Makinde [21], Adesanya and Makinde [22], Mkwizu and Makinde [23], Eegunjobi and Makinde [24] Butt *et al.* [25] and Munawar *et al.* [26]) who explored the phenomenon of entropy in convective heat transfer problems under various physical assumptions. Despite of all the work done we found a very few studies in which the entropy of a biological system has been examined. In this regard, Souidi *et al.* [27] calculated the entropy production for a peristaltic pump and in a contracting tube. Entropy generation in peristaltic flow of nanofluid in a non-uniform channel with compliant walls was examined by Abbas *et al.* [28]. Recently, Munawar *et al.* [29] investigated the second-law in a peristaltic flow of variable viscosity fluid and revealed that entropy production is high in the contracted region and reduces in the wider part of channel.

In this article we aim to examine the entropy production in a peristaltic flow of a viscous fluid with space dependent viscosity in an asymmetric channel. Heat transfer and fluid friction irreversibilities are assumed to be the main factors of entropy production. The governing equations are modeled in the wave frame and simplified under the assumptions of long wavelength and the small Reynolds number. Exact solutions are calculated for the dimensionless linear governing equations. The entropy expression is calculated by using the solutions and then a brief analysis is carried out using graphical results.

2. Mathematical formulation

Consider two-dimensional peristaltic motion of an incompressible viscous fluid in an asymmetric channel. The flow is produced due to sinusoidal waves travelling along the channel wall with constant speed c. Using a rectangular coordinate system, x-axis is taken along the direction of wave propagation and y-axis is normal to it. Moreover, the upper and the lower walls are kept at uniform temperatures of T_1 and T_2, respectively and it is assumed that $T_2 > T_1$. The equations of wall in moving frame are defined as:

$$h_1^* = d_1 + a\sin\left(\frac{2\pi x^*}{\lambda}\right), \tag{1}$$

$$h_2^* = d_2 + b\sin\left(\frac{2\pi x^*}{\lambda} + \phi\right), \tag{2}$$

where $d_1 + d_2$ is the channel width, a_1 and a_2 amplitudes of the wave, λ is the wavelength, and ϕ is the phase difference which varies in the range $0 < \phi \le \pi$. It is to be noted that for $\phi = \pi$ both the waves are in phase (see for instance, Fig. 1). The dimensional governing equations in wave frame of reference are:

$$\frac{\partial u^*}{\partial x^*} + \frac{\partial v^*}{\partial y^*} = 0, \tag{3}$$

$$\rho\left(u^*\frac{\partial}{\partial x^*} + v^*\frac{\partial}{\partial y^*}\right)u^* = -\frac{\partial p^*}{\partial x^*} + 2\frac{\partial}{\partial x^*}\left\{\mu^*\left(y^*\right)\frac{\partial u^*}{\partial x^*}\right\} + \frac{\partial}{\partial y^*}\left\{\mu^*\left(y^*\right)\left(\frac{\partial u^*}{\partial y^*} + \frac{\partial v^*}{\partial x^*}\right)\right\}, \tag{4}$$

$$\rho\left(u^*\frac{\partial}{\partial x^*} + v^*\frac{\partial}{\partial y^*}\right)v^* = -\frac{\partial p^*}{\partial y^*} + 2\frac{\partial}{\partial y^*}\left\{\mu^*\left(y^*\right)\frac{\partial v^*}{\partial y^*}\right\} + \frac{\partial}{\partial x^*}\left\{\mu^*\left(y^*\right)\left(\frac{\partial v^*}{\partial x^*} + \frac{\partial u^*}{\partial y^*}\right)\right\}, \tag{5}$$

$$\rho C_p\left(u^*\frac{\partial T}{\partial x^*} + v^*\frac{\partial T}{\partial y^*}\right) = k\left(\frac{\partial^2 T}{\partial x^{*2}} + \frac{\partial^2 T}{\partial y^{*2}}\right) + \mu^*\left(y^*\right)\left\{\left(\frac{\partial u^*}{\partial x^*}\right)^2 + \left(\frac{\partial u^*}{\partial y^*} + \frac{\partial v^*}{\partial x^*}\right)^2 + \left(\frac{\partial v^*}{\partial y^*}\right)^2\right\}. \tag{6}$$

The dimensionless quantities are defined as

$$\begin{cases} x=\dfrac{x^*}{\lambda}, y=\dfrac{y^*}{d_1}, u=\dfrac{u^*}{c}, v=\dfrac{v^*}{c}, t=\dfrac{t'c}{\lambda}, h_1=\dfrac{h_1^*}{d_1}, h_2=\dfrac{h_2^*}{d_1},\ \delta=\dfrac{d_1}{\lambda}, a=\dfrac{a_1}{d_1}, \\ b=\dfrac{a_2}{d_1}, d=\dfrac{d_2}{d_1}, \mu=\dfrac{\mu^*}{\mu_0}, Re=\dfrac{cd_1}{\nu}, Pr=\dfrac{\mu C_p}{k}, Er=\dfrac{c^2}{C_p\left(T_2-T_1\right)}, \\ \Psi=\dfrac{\Psi^*}{cd_1}, u=\dfrac{\partial\Psi}{\partial y}, v=-\dfrac{\partial\Psi}{\partial x}, p=\dfrac{d_1{}^2 p^*}{c\lambda\mu_0}, \theta=\dfrac{T-T_1}{T_2-T_1}. \end{cases} \tag{7}$$

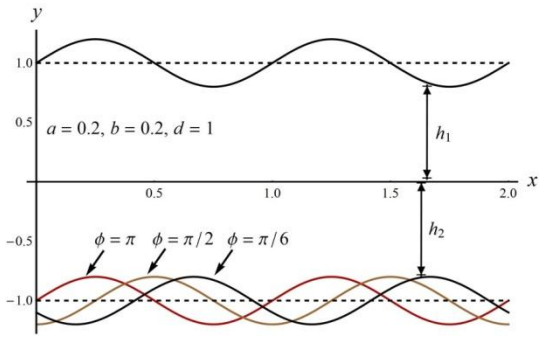

Figure 1: Schematic diagram of the flow phenomenon

Using the above mentioned quantities (7), Eqs. (1)-(6) take the form

$$h_1\left(x\right)=1+a\sin\left(2\pi x\right), \tag{8}$$

$$h_2\left(x\right)=d+b\sin\left(2\pi x+\phi\right), \tag{9}$$

$$Re\delta\left(\frac{\partial\Psi}{\partial y}\frac{\partial^2\Psi}{\partial x\partial y}-\frac{\partial\Psi}{\partial x}\frac{\partial^2\Psi}{\partial y^2}\right)=-\frac{\partial p}{\partial x}+2\delta^2\frac{\partial}{\partial x}\left(\mu\left(y\right)\frac{\partial^2\Psi}{\partial x\partial y}\right)+\frac{\partial}{\partial y}\left[\mu\left(y\right)\left(\frac{\partial^2\Psi}{\partial y^2}-\delta^2\frac{\partial^2\Psi}{\partial x^2}\right)\right], \tag{10}$$

$$Re\delta^2\left(\frac{\partial\Psi}{\partial y}\frac{\partial^2\Psi}{\partial x^2}-\delta\frac{\partial\Psi}{\partial x}\frac{\partial^2\Psi}{\partial x\partial y}\right)=\frac{\partial p}{\partial y}+2\delta^2\frac{\partial}{\partial y}\left(\mu\left(y\right)\frac{\partial^2\Psi}{\partial x\partial y}\right)-\delta^2\frac{\partial}{\partial x}\left[\mu\left(y\right)\left(\frac{\partial^2\Psi}{\partial y^2}-\delta^2\frac{\partial^2\Psi}{\partial x^2}\right)\right], \tag{11}$$

$$Re\delta\left(\frac{\partial\Psi}{\partial y}\frac{\partial\theta}{\partial x}-\frac{\partial\Psi}{\partial x}\frac{\partial\theta}{\partial y}\right)=\frac{1}{\mathrm{Pr}}\left(\delta^2\frac{\partial^2\theta}{\partial x^2}+\frac{\partial^2\theta}{\partial y^2}\right)+\mathrm{Er}\mu\left(y\right)\left[2\delta^2\left(\frac{\partial^2\Psi}{\partial x\partial y}\right)^2+\left(\frac{\partial^2\Psi}{\partial y^2}-\delta^2\frac{\partial^2\Psi}{\partial x^2}\right)^2\right], \tag{12}$$

where Er is the Eckert number, Pr the Prandtl number, δ the wave number and *Re* the Reynolds number, μ_0 the viscosity at endoscope, Ψ the stream function and T_1, and T_2 are temperatures at $y = h_1$ and $y = h_2$, respectively. The viscosity of fluid is assumed to be space dependent as proposed by Srivastava *et al.* [30] and is described by

$$\mu\left(y\right)=e^{-\alpha y}\quad \text{for}\quad \alpha\ll 1\ \text{or}\ \ \mu\left(y\right)\approx 1-\alpha y, \tag{13}$$

where α is the viscosity parameter. Assuming the long wavelength and low Reynolds number Eqs. (10)-(12) take the form

$$\frac{\partial p}{\partial x} = \frac{\partial}{\partial y}\left((1-\alpha y)\frac{\partial^2 \Psi}{\partial y^2} \right), \tag{14}$$

$$\frac{\partial p}{\partial y} = 0, \tag{15}$$

$$\frac{\partial^2 \theta}{\partial y^2} + (1-\alpha y)\,\mathrm{Br}\left(\frac{\partial^2 \Psi}{\partial y^2} \right)^2 = 0, \tag{16}$$

where Br = PrEr is the Brinkman number. With the aid of Eqs. (14) and (15) one gets,

$$\frac{\partial^2}{\partial y^2}\left((1-\alpha y)\frac{\partial^2 \Psi}{\partial y^2} \right) = 0. \tag{17}$$

The dimensionless boundary conditions and pressure rise per wavelength Δp_λ are noted as

$$\Psi = \frac{F}{2},\ \frac{\partial \Psi}{\partial y} = -1, \quad \theta = 0 \ \text{ at } \ y = h_1, \tag{18}$$

$$\Psi = -\frac{F}{2},\ \frac{\partial \Psi}{\partial y} = -1,\ \theta = 1 \text{ at } \quad y = h_2, \tag{19}$$

$$\Delta P_\lambda = \int_0^1 \left(\frac{dp}{dx} \right) dx, \tag{20}$$

and

$$\Theta = 1 + F + d. \tag{21}$$

The solutions of Eqs. (14)-(17) subject to the boundary conditions (18) and (19) can be found easily by using the command "DSolve" of the symbolic computational software Mathematica. To validate the analytic results, we have also obtained the numerical solutions (by shooting method) and the comparison of results by both techniques has been reported in Table 1. The table shows a good agreement between analytical and numerical solutions.

Table 1: Comparison of analytical results with the results by numerical shooting method for skin friction at upper and lower walls when $\Theta = 1$, $a = b = 0.2$, x = 0.5, $\phi = \pi/3$

α	$\Psi''(h_1)$ (Analytic)	$\Psi''(h_1)$ (Numerical)	$\Psi''(h_2)$ (Analytic)	$\Psi''(h_2)$ (Numerical)
0.1	-5.41353405	-5.41353345	4.78596063	4.78596068
0.2	-5.79801682	-5.79801688	4.51137917	4.51137918
0.3	-6.25629214	-6.25629222	4.25295278	4.25295268
0.4	-6.82079823	-6.82079840	4.00566049	4.00566053
0.5	-7.54687042	-7.54687061	3.76457591	3.76457584

3. Entropy Analysis

The entropy production in the peristaltic flow can be examined by using the following expression of total volumetric local rate of entropy generation in moving frame:

$$S'''_{gen} = \frac{k}{T_1^2}\left[\left(\frac{\partial T}{\partial x^*}\right)^2 + \left(\frac{\partial T}{\partial y^*}\right)^2\right] + \frac{\mu^*\left(y^*\right)}{T_1}\left[2\left(\frac{\partial u^*}{\partial x^*}\right)^2 + 2\left(\frac{\partial v^*}{\partial y^*}\right)^2 + \left(\frac{\partial v^*}{\partial x^*} + \frac{\partial u^*}{\partial y^*}\right)^2\right]. \tag{22}$$

It is assumed that the entropy in the system is produced due to heat transfer and fluid friction. using Eq. (7) and divided the above equation with characteristic entropy (S_{G0}), one gets the total entropy generation number (N_G) as

$$N_G = \tau\left(\frac{\partial \theta}{\partial y}\right)^2 + Br\left(1-\alpha y\right)\left(\frac{\partial^2 \Psi}{\partial y^2}\right)^2, \tag{23}$$

where $\tau = \Delta T/T_1$ is the dimensionless temperature difference (we set $\tau = 1$). The first term in Eq. (23) denotes the irreversibility due to heat transfer and the second term represents the fluid friction irreversibility. The average entropy generation number is given by

$$Ns_{avg} = \frac{1}{\forall}\int_0^1\int_{h_2}^{h_1} N_G\, dy dx, \tag{24}$$

where $\forall = 2$ is the area of the integrated region between $x = 0$ and $x = 1$. To see the discriminating effects of fluid friction irreversibility over the heat transfer irreversibility the Bejan number is introduced as

$$Be = \frac{1}{1+\Phi}, \tag{25}$$

and

$$\Phi = Br\left(1-\alpha y\right)\left(\frac{\partial^2 \Psi}{\partial y^2}\right)^2 \Big/ \tau\left(\frac{\partial \theta}{\partial y}\right)^2, \tag{26}$$

where Φ is the irreversibility distribution ratio. The Bejan number *Be* is bounded between the range [0, 1]. The Bejan number greater than 0.5 represents the dominancy of heat transfer irreversibility over fluid friction irreversibility, whereas, for the Bejan number less than 0.5 fluid friction irreversibility dominates.

4. Results and discussion

To see the effects of various physical parameters on various quantities of interest figures 2-14 are plotted. In Fig. 2 the pressure difference per wavelength ΔP_λ and the pressure variation dp/dx are plotted for different values of parameter α. It is noted from Fig. 2 that in both the retrograde pumping region ($\Theta < 0$, $\Delta P_\lambda > 0$) and in the augmented pumping region ($\Theta > 0$, $\Delta P_\lambda < 0$) the pressure differences per wavelength ΔP_λ decreases as α increases. From here it is noticed that the pressure difference in the

variable viscosity fluid is greater than the case of constant viscosity fluid. Moreover Fig. 2 discloses that in the reverse flow situation ($\Theta = -1$), as α increases, the adverse pressure gradient decreases. Though, this decrease is more significant in the narrow region ($0.5 < \phi < 0.9$ roughly) of the channel. Such sort of result is quite expected due to decreasing fluid frictional force. Moreover, the pressure gradient is large in the narrow region or, in other words, in order to maintain the same flux ($\Theta = -1$) in the contracted part a larger adverse pressure gradient ($dp/dx > 0$) is needed as compared to the expanded region.

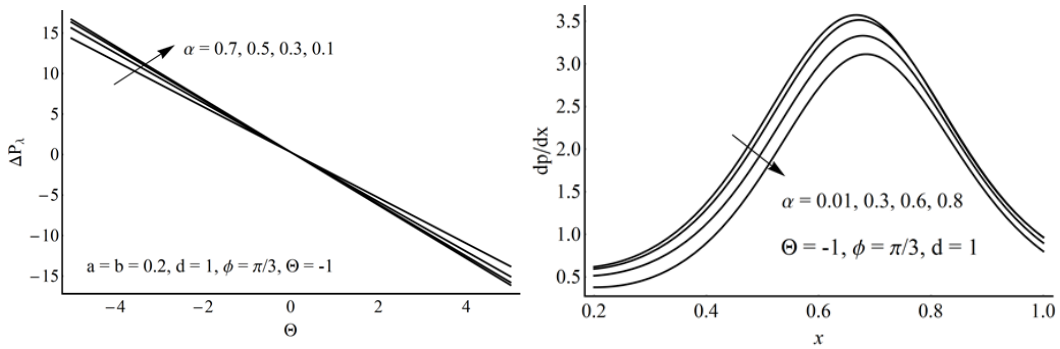

Figure 2: Pressure drop and gradient for different values of variable α

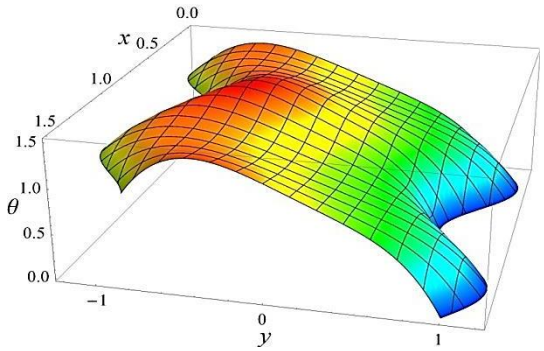

Figure 3: A 3D view of velocity profile when $\alpha = 0.4$, Br = 0.4, $a = b = 0.2$, $d = 1$, $\phi = \pi/3$ and $\Theta = 3$

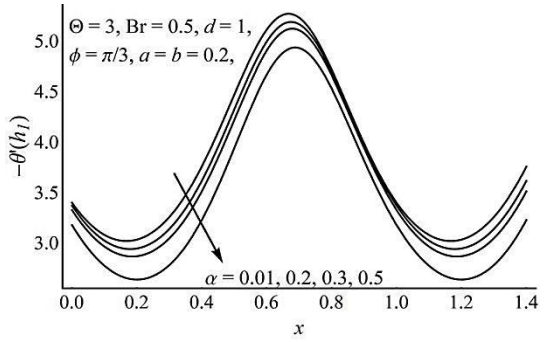

Figure 4: Heat transfer rate against variable x for different values of α

Fig. 3 demonstrates a 3D view of the temperature profile against dimensionless x and y-coordinates. The temperature profile is high in the narrow part of the channel and is low near the wider part. This is due to the large fluid fiction effects in the narrow part for which extensive internal heat generation produced. Consequently, the heat transfer rate in the narrow part ($0.5 < x < 0.9$ roughly) is

high as compared to the wider part (See for instance Fig. 4). Moreover, Fig. 4 also shows that the heat transfer rate at the upper wall decreases as the parameter α increases which is due to the poor thermal conductance. This shows that the fluids with greater α values are good for thermal insulation problems.

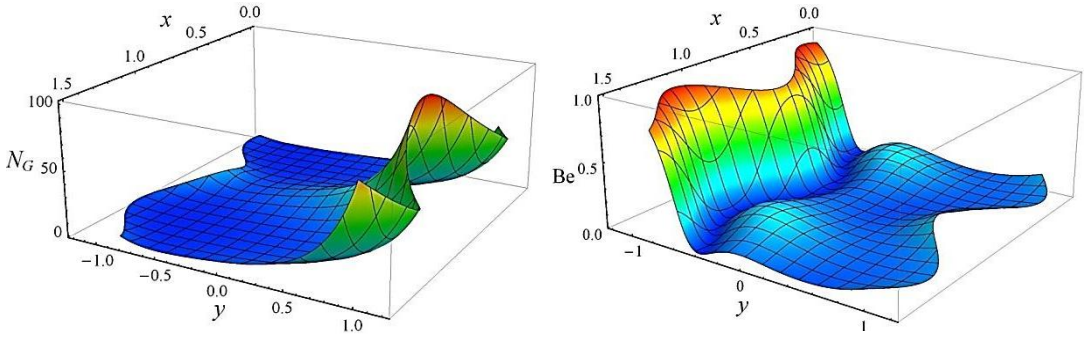

Figure 5: A 3D view of the entropy generation and the Bejan number when α = 0.4, Br = 0.4, $a = b$ = 0.2, d = 1, $\phi = \pi/3$ and Θ = 3

A 3-D view of total entropy number and Bejan number against the dimensionless x and y-coordinates is demonstrated in Fig. 5. It is noted that the entropy is higher near the cold wall (at $y = h_1$) as compared to the heated wall (at $y = h_2$) of the channel. This is due to large temperature gradient near the cold wall of the channel ($y = h_1$). It is further observed that the entropy is relatively maximum at the narrow part of the channel and minimum at the wider part. From the figure it can be seen that near the cold wall of the channel fluid friction irreversibility dominates, however, near the heated wall irreversibility is dominated by the heat transfer effects. Moreover, in the narrow part of the channel a decreasing trend is noticed in the irreversibility due to heat transfer near the heated wall. Fig. 6 reveals that as the parameter α increases the total entropy generation number N_G also increases and the increase is more significant near the cold wall. However, the fluid friction irreversibility dominates near cold wall as α increases (see for instance Fig. 7). Such type of results were not noticed in case of symmetric channel (see Munawar *et al.* [29]) where entropy decreases with the increase of α. However, in both cases, either symmetric or asymmetric, entropy generation due to heat transfer reduces as α increases which shows poor thermal conductance of fluids have large α values. Here the increase in the total entropy generation might be due to the asymmetric nature of the channel and space dependent variable viscosity.

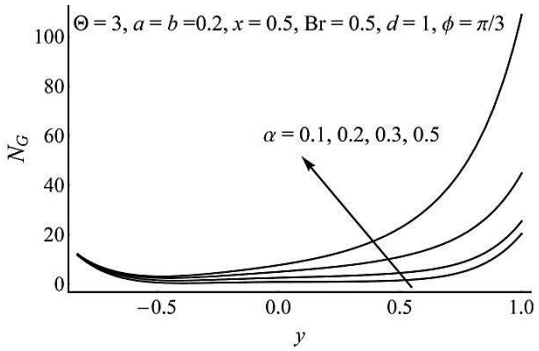

Figure 6: Effect of parameter α on entropy generation number

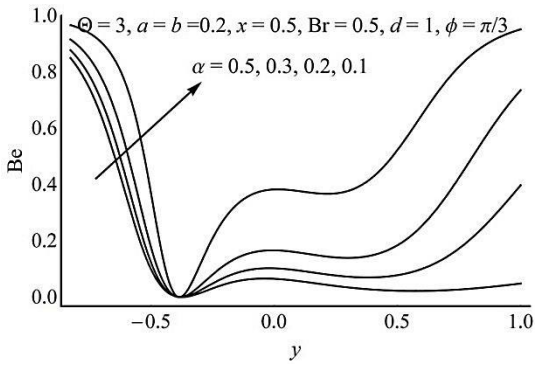

Figure 7: Effect of parameter α on the Bejan number

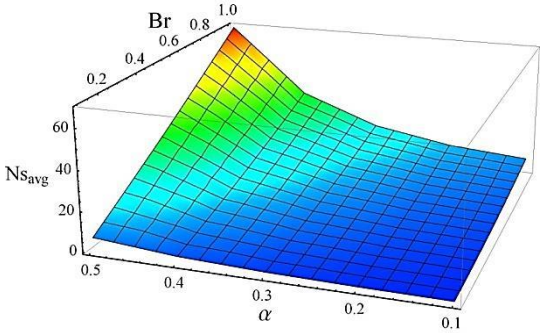

Figure 8: A 3D view of the average entropy against α and Br when $a = b = 0.2$, $d = 1$, $\phi = \pi/3$ and $\Theta = 3$

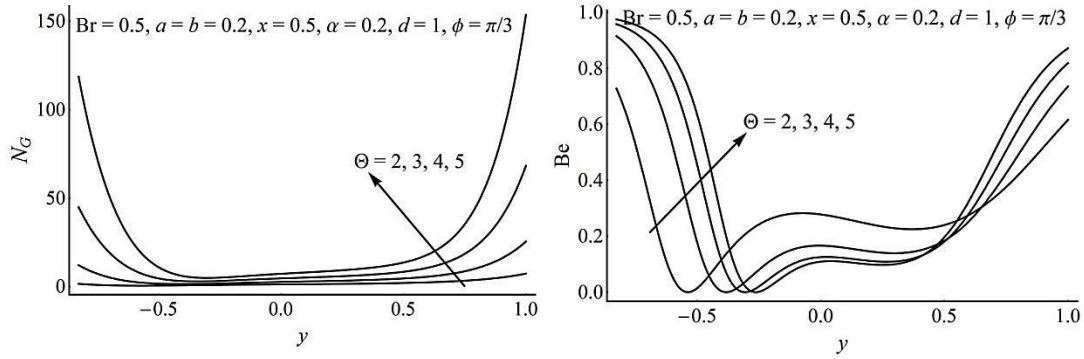

Figure 9: Effect of mass flow rate Θ on entropy generation number N_G and the Bejan number Be

Fig. 8 unveils the average entropy generation number Ns_{avg} in a 3-D configuration against α and Br. It is observed that the average entropy of the channel increases as Br and α increase. Therefore minimum entropy can be obtained if the Brinkman number Br and the parameter α are kept small. Fig. 9 reveals that as the flow rate parameter Θ increases the entropy production rises significantly near both the walls. Moreover, it is also shown in Fig. 9 that as Θ increases the entropy is controlled by heat transfer effects near the walls and by the fluid friction effects in the center of the channel. This is quietly expected result because as the flow rate increases the heat transfer rate also augments with fluid particles which results in the entropy enhancement.

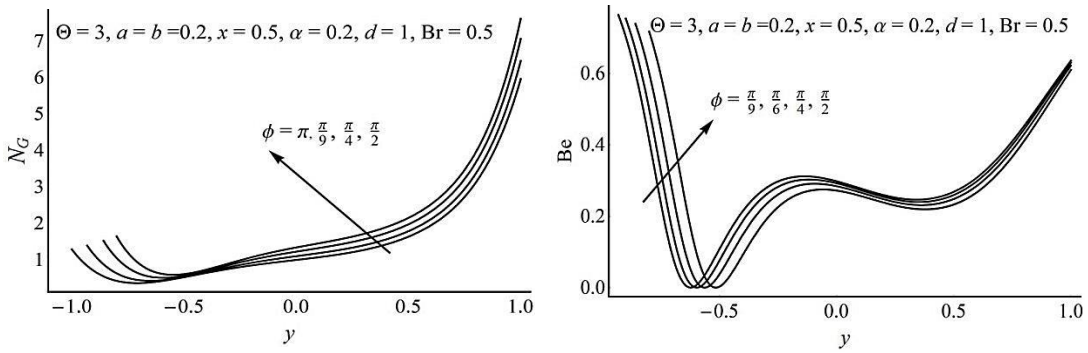

Figure 10: Effect of phase difference ϕ on the entropy generation number N_G and the Bejan number Be

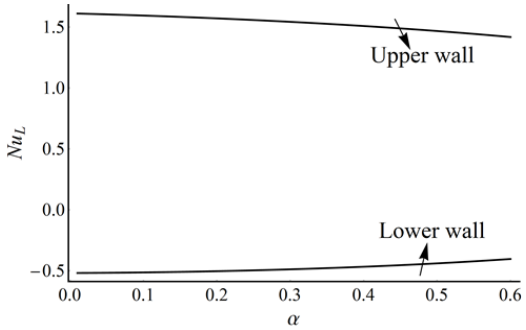

Figure 11: The Nusselt number at both walls of the channel against α

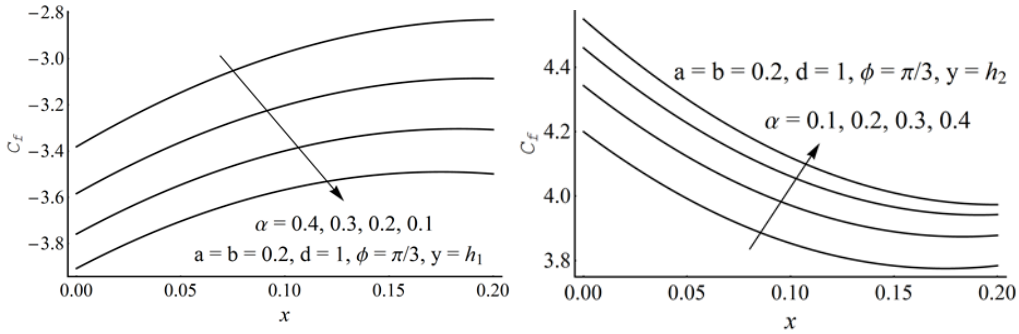

Figure 12: Skin friction at the upper and lower walls for different values of α

From Fig. 10 it is observed that the entropy generation is minimum when both the waves are in phase ($\phi = \pi$) and it increases as the phase changes. Fig. 10 also shows that the entropy due to heat transfer is dominant near both the walls; however, it decreases at lower wall when waves are in phase and it increases near upper wall when waves shifted to be in phase. The Nusselt number versus variable viscosity parameter is plotted at the upper and lower channel wall in Fig. 11. From this figure it is clear that magnitude of Nu_L decreases for large values of α. Skin friction at upper and lower channel boundaries can be seen through Fig. 12. It is observed that the magnitude of skin friction increases with an increase in α.

5. Conclusion

A complete thermo-dynamical analysis has been made for a peristaltic flow of a variable viscosity fluid in an asymmetric channel. The isothermal boundary conditions are used for the heated walls of the channel and exact solutions have been calculated. It is concluded that the temperature as well as the entropy of fluid is high in the narrow parts of the channel. Also entropy is high near the cooler wall of the channel and is low near the hotter wall. Moreover, it is established that in the fluids having higher values of the parameter α, the average entropy is high. To minimize average entropy of the system the viscous dissipation and the value of α should be kept small.

References

[1] Latham, T. W., Fluid motions in a peristaltic pump., Massachusetts Institute of Technology, Cambridge, Massachusetts, USA, (1966)

[2] Shapiro, A. H. *et al.*, Peristaltic pumping with long wavelengths at low Reynolds number, *Journal of Fluid Mechanics*, 37 (1969), 04, pp. 799-825

[3] Eytan, O., Elad, D., Analysis of intra-uterine fluid motion induced by uterine contractions, *Bulletin of Mathematical Biology*, 61 (1999), 2, pp. 221-238

[4] Srinivas, S., Pushparaj, V., Non-linear peristaltic transport in an inclined asymmetric channel, *Communications in Nonlinear Science and Numerical Simulation*, 13 (2008), 9, pp. 1782-1795

[5] Naga Rani, P., Sarojamma, G., Peristaltic transport of a Casson fluid in an asymmetric channel, *Australasian Physics & Engineering Sciences in Medicine*, 27 (2004), 2, pp. 49-59

[6] Mishra, M., Rao, A. R., Peristaltic transport of a Newtonian fluid in an asymmetric channel, *Zeitschrift für angewandte Mathematik und Physik ZAMP*, 54 (2003), 3, pp. 532-550

[7] Hayat, T. *et al.*, Slip and heat transfer effects on peristaltic motion of a Carreau fluid in an asymmetric channel, *Zeitschrift Fur Naturforschung Section A-A Journal of Physical Sciences*, 65a (2010), pp. 1121-1127

[8] Sarkar, B. C. *et al.*, Magnetohydrodynamic peristaltic flow of nanofluids in a convectively heated vertical asymmetric channel in presence of thermal radiation, *Journal of Nanofluids*, 4 (2015), 4, pp. 461-473

[9] Akbar, N. S. *et al.*, Modeling nanoparticle geometry effects on peristaltic pumping of medical magnetohydrodynamic nanofluids with heat transfer, *Journal of Mechanics in Medicine and Biology*, 16 (2016), 06, pp. 1650088

[10] Sher Akbar, N. *et al.*, Thermally developing MHD peristaltic transport of nanofluids with velocity and thermal slip effects, *The European Physical Journal Plus*, 131 (2016), 9, pp. 332

[11] Bejan, A., A study of entropy generation in fundamental convective heat transfer, *Journal of Heat Transfer-Transactions of the ASME*, 101 (1979), 4, pp. 718-725

[12] Bejan, A., Second law analysis in heat transfer, *Energy*, 5 (1980), 8–9, pp. 720-732

[13] Bejan, A., *Entropy Generation Minimization*, CRC Press, Boca Raton, New York, 1996

[14] Arikoglu, A. *et al.*, Effect of slip on entropy generation in a single rotating disk in MHD flow, *Applied Energy*, 85 (2008), 12, pp. 1225-1236

[15] Tamayol, A. *et al.*, Thermal analysis of flow in a porous medium over a permeable stretching wall, *Transport in Porous Media*, 85 (2010), 3, pp. 661-676
[16] Butt, A. S. *et al.*, Slip effects on entropy generation in MHD flow over a stretching surface in the presence of thermal radiation, *International Journal of Exergy*, 13 (2013), 1, pp. 1-20
[17] Erbay, L. *et al.*, Entropy Generation During Fluid Flow Between Two Parallel Plates With Moving Bottom Plate, *Entropy*, 5 (2003), 5, pp. 506-518
[18] Abu-Hijleh, B. A. K., Heilen, W. N., Entropy generation due to laminar natural convection over a heated rotating cylinder, *International Journal of Heat and Mass Transfer*, 42 (1999), 22, pp. 4225-4233
[19] Tasnim, S. H. *et al.*, Entropy generation in a porous channel with hydromagnetic effect, *Exergy, An International Journal*, 2 (2002), 4, pp. 300-308
[20] Eegunjobi, A. S. *et al.*, Irreversibility analysis of unsteady couette flow with variable viscosity, *Journal of Hydrodynamics, Ser. B*, 27 (2015), 2, pp. 304-310
[21] Adesanya, S. O., Makinde, O. D., Thermodynamic analysis for a third grade fluid through a vertical channel with internal heat generation, *Journal of Hydrodynamics, Ser. B*, 27 (2015), 2, pp. 264-272
[22] Adesanya, S. O., Makinde, O. D., Irreversibility analysis in a couple stress film flow along an inclined heated plate with adiabatic free surface, *Physica A: Statistical Mechanics and its Applications*, 432 (2015), 0, pp. 222-229
[23] Mkwizu, M. H., Makinde, O. D., Entropy generation in a variable viscosity channel flow of nanofluids with convective cooling, *Comptes Rendus Mécanique*, 343 (2015), 1, pp. 38-56
[24] Eegunjobi, A. S., Makinde, O. D., Irreversibility analysis of hydromagnetic flow of couple stress fluid with radiative heat in a channel filled with a porous medium, *Results in Physics*, 7 (2017), pp. 459-469
[25] Butt, A. S. *et al.*, Entropy analysis of mixed convective magnetohydrodynamic flow of a viscoelastic fluid over a stretching sheet, *Zeitschrift Fur Naturforschung Section A-A Journal of Physical Sciences*, 67 (2012), 8-9, pp. 451-459
[26] Munawar, S. *et al.*, Thermal analysis of the flow over an oscillatory stretching cylinder, *Physica Scripta*, 86 (2012), 6, 065401 pp. 065401
[27] Souidi, F. *et al.*, Entropy generation rate for a peristaltic pump, *Journal of Non-Equilibrium Thermodynamics*, 34 (2009), 2, pp. 171-194
[28] Abbas, M. *et al.*, Analysis of Entropy Generation in the Flow of Peristaltic Nanofluids in Channels With Compliant Walls, *Entropy*, 18 (2016), 3, pp. 90
[29] Munawar, S. *et al.*, Second law analysis in the peristaltic flow of variable viscosity fluid, *International Journal of Exergy*, 20 (2016), 2, pp. 170-185
[30] Srivastava, L. M. *et al.*, Peristaltic transport of a physiological fluid. Part I. Flow in non-uniform geometry, *Biorheology*, 20 (1983), 2, pp. 153-166